MICROBIOLOGY

In situ diversity of metabolism and carbon use efficiency among soil bacteria

Weichao Wu[1,2,3]*, Paul Dijkstra[4], Bruce A. Hungate[4], Lingling Shi[5,6,7], Michaela A. Dippold[1,7]

The central carbon (C) metabolic network harvests energy to power the cell and feed biosynthesis for growth. In pure cultures, bacteria use some but not all of the network's major pathways, such as glycolysis and pentose phosphate and Entner-Doudoroff pathways. However, how these pathways are used in microorganisms in intact soil communities is unknown. Here, we analyzed the incorporation of ^{13}C from glucose isotopomers into phospholipid fatty acids. We showed that groups of Gram-positive and Gram-negative bacteria in an intact agricultural soil used different pathways to metabolize glucose. They also differed in C use efficiency (CUE), the efficiency with which a substrate is used for biosynthesis. Our results provide experimental evidence for diversity among microbes in the organization of their central carbon metabolic network and CUE under in situ conditions. These results have important implications for our understanding of how community composition affects soil C cycling and organic matter formation.

INTRODUCTION

Microbes are fundamental drivers of soil ecosystem processes. Carbon use efficiency (CUE) is a key parameter in modeling of soil carbon (C) cycling (*1*). The value of CUE describes how much microbial biomass is produced per substrate consumed and thus affects how much carbon can be stored as potentially long-term stabilized soil organic matter versus how much is released as CO_2. Understanding the underlying mechanisms that drive CUE is essential for understanding how soil ecosystems function and respond to environmental change (*2*). CUE, as is often measured, not only reflects energy needs for growth and cell maintenance but also integrates the effects of variation in exudation of metabolites, extracellular enzymes, and microbial death (*3*, *4*). Here, we use ^{13}C metabolic flux analysis and modeling to estimate the efficiency of the biochemical processes of the central C metabolic network, responsible for most of the energy and CO_2 produced in heterotrophic microbes under in situ conditions in an intact, complex soil community.

The central C metabolic network, consisting of Embden-Meyerhof-Parnas glycolysis and pentose phosphate and Entner-Doudoroff pathways, as well as the downstream tricarboxylic acid cycle, has been extensively studied in microbial isolates under laboratory conditions (*5*–*8*). Recently, large-scale genome-informed modeling of the central C metabolic processes and CUE has been done, including for species that cannot be cultured (*9*–*11*). However, these genomic analyses may not capture in situ microbial metabolism and CUE in complex microbial communities because of the strong influence of environmental conditions (e.g., temperature, pH, and nutrients) on microbial activity and CUE (*1*, *10*, *12*).

The position-specific ^{13}C-CO_2 production from glucose isotopomers has been used to model metabolism and CUE for intact soil ecosystems (*2*, *13*). These measurements reflect metabolism and efficiency averaged across the entire soil microbial community. This approach does not differentiate between individual organisms or groups of organisms within that community as CO_2, the target metabolic product of that approach, is jointly produced by the entire heterotrophic soil community.

^{13}C incorporation from labeled compounds into signature molecules, e.g., phospholipid fatty acids (PLFAs), can differentiate among groups of soil organisms (*14*, *15*), for example, in their uptake of glucose (*16*, *17*). The PLFA technique has been used for microbial community characterization for several decades (*15*, *18*, *19*). This method divides the microbial community into large groups (e.g., Gram-positive bacteria) on the basis of characteristic profiles of PLFAs (*18*, *19*). This does not mean that microorganisms outside this group do not produce these fatty acids nor that each Gram-negative bacterium produces only this PLFA, just that Gram-negative bacteria as a group produce most of that PLFA in the soil community. By tracing different isotopomers of ^{13}C-glucose into signature molecules, it should be possible to perform soil fluxomics and model the activity of the central C metabolic network and CUE for groups of organisms within an intact soil community.

Wu *et al.* (*20*) developed a technique to analyze the ^{13}C incorporation from position-specific ^{13}C-labeled glucose isotopomers into ethanoate and propionate fragments from individual PLFAs. These fragments are derived from acetyl–coenzyme A (acetyl-CoA), and the two carbon atoms from the acetyl unit are preserved in PLFA synthesis. Therefore, these fragments can be used to model the central C metabolic network for the organisms that produce these signature lipids. The main goal of this study is to identify how groups of organisms within a community use the central C metabolic network and to estimate the efficiency of glucose use under in situ, intact soil conditions. These measurements will help us understand the roles of individual community members in whole soil metabolic activities, CUE, respiration, and potentially necromass formation and soil organic matter formation.

We used an agricultural soil and incubated it with six ^{13}C-glucose isotopomers in parallel incubations, extracted PLFAs, and analyzed

[1]Biogeochemistry of Agroecosystem, University of Goettingen, Goettingen, Germany. [2]Department of Environmental Science, Stockholm University, Stockholm, Sweden. [3]Shanghai Engineering Research Center of Hadal Science and Technology, College of Marine Science, Shanghai Ocean University, Shanghai, China. [4]Center for Ecosystem Science and Society and Department of Biological Sciences, Northern Arizona University, Flagstaff, AZ, USA. [5]Key Laboratory of Economics Plants and Biotechnology, Institute of Botany, Chinese Academy of Sciences, Kunming, China. [6]World Agroforestry Centre, China and East-Asia Office, Kunming, China. [7]Geo-Biosphere Interactions, Department of Geosciences, University of Tuebingen, Tuebingen, Germany. *Corresponding author. Email: wwcpku@gmail.com

the ethanoate and propionate fragments using a conventional electron-impact gas chromatography–mass spectrometer (GC-MS) (for details, see Materials and Methods) following Wu *et al.* (*20*). The results for this one soil indicate the diversity of metabolic processes and CUE within an intact soil community, confirming genomics observations and long-held assumptions in soil C cycling modeling (*21*).

RESULTS

Positional ^{13}C incorporation into PLFAs

We detected 27 PLFAs in our soil samples of which bacterial PLFAs accounted for 96 ± 0.6% and fungal PLFAs ($C_{18:2\omega6,9}$) for 1.95 ± 0.06%, suggesting a low fungal biomass in this agricultural soil, compared to, for example, >10% for a forest soil [also see the Supplementary Materials; (*22*)]. As a result, our analysis is focused on bacteria only. We analyzed ethanoate and propionate fragments of 16 bacterial PLFAs (including straight, monounsaturated, iso, and anteiso; Supplementary Materials) making up 80% of extracted PLFAs. We have shown proof of concept of this measurement of fragment enrichment of these PLFAs and modeled metabolic organization using pure cultures of *Bacillus licheniformis* and *Pseudomonas fluorescens* (*20*). In soil, all ^{13}C glucose isotopomer additions resulted in significant ^{13}C incorporation into PLFAs compared to the control with glucose with natural abundance isotope composition (Fig. 1). As expected, the ^{13}C enrichment differed between glucose isotopomers (Fig. 1 and Supplementary Materials). Glucose-5-^{13}C and glucose-6-^{13}C yielded higher ^{13}C enrichment than other ^{13}C isotopomers. Propionate showed a higher ^{13}C enrichment than ethanoate [repeated measures analysis of variance (ANOVA), df = 15,2, $F = 42.2$; $P < 0.001$; Fig. 1] when incubated with glucose-5-^{13}C but a lower enrichment when incubated with glucose-6-^{13}C (repeated-measures ANOVA, df = 15,2, $F = 17.6$; $P < 0.001$; Fig. 1). The difference in ^{13}C incorporation between ethanoate and propionate fragments was also observed when incubated with glucose-1-^{13}C and glucose-2-^{13}C (Fig. 1).

Regardless of the metabolic pathways, carbon atoms from positions 5 and 6 of the glucose molecule are consistently incorporated into PLFAs during biosynthesis, and carbon atom from position 4 is consistently lost as CO_2 (Fig. 2). In contrast, whether carbon atoms from positions 1, 2, and 3 from glucose end up in PLFAs depends strongly on the metabolic pathway (Fig. 2). Further details of metabolic organization, for example, the rate of anaplerotic reactions and the citric acid pathway, can be identified from the pattern of C4, C5, and C6. The incorporation patterns were used to model the metabolic flux pathways used by the organisms that produced the different fatty acids.

Organization of metabolism as a function of PLFAs and microbial identity

To estimate the flux rates through the pathways of the central C metabolic network (fig. S1), we used a model consisting of 18 reactions and eight biomass functions (*20*) with precursor demand following Dijkstra *et al.* (table S1) (*4*, *13*). The observed labeling patterns corresponded to significant differences in the biochemical pathways that were involved in producing these PLFAs (Fig. 3 and table S2). The nonmetric multidimensional scaling (NMDS) and cluster analysis of PLFA-based metabolic fluxes distinguish at least three groups of PLFAs on the basis of their metabolic organization (Fig. 3A). Branched PLFAs were part of two groups (clusters A and B), whereas unsaturated PLFAs were associated with cluster C. PLFAs in clusters A and B showed high pentose phosphate pathway activity, while PLFAs in cluster C partition glucose equally over pentose phosphate and Entner-Doudoroff pathways (Fig. 4A). The universal PLFAs such as straight and saturated C_{15}, C_{16}, and C_{17} fatty acids were part of cluster C, suggesting that the overall microbial community share similar metabolic flux patterns as the other PLFAs in cluster C.

We assigned branched PLFAs (clusters A and B) as Gram-positive bacteria and unsaturated PLFAs (cluster C) as Gram-negative bacteria (Fig. 3B) following Zelles (*14*), Frostegård *et al.* (*15*), and Joergensen (*19*). Cluster A consisted of branched PLFAs, supporting an origin

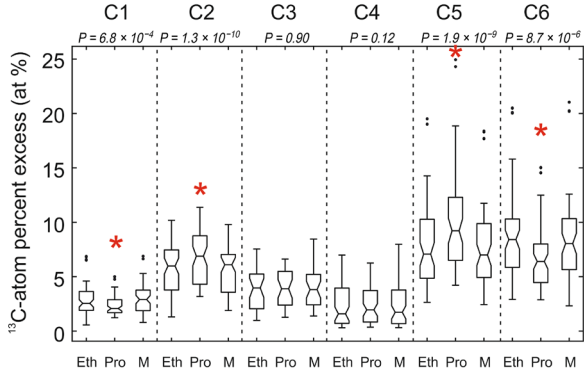

Fig. 1. Atom percent excess enrichment of ^{13}C of fragment and entire molecule of PLFAs (C_{14} to C_{18}) after a 10-day incubation with position-specific ^{13}C-labeled glucose. Fragments include ethanoate (Eth), propionate (Pro), and the molecular ion (M). C1 to C6 refer to glucose-1-^{13}C, glucose-2-^{13}C, glucose-3-^{13}C, glucose-4-^{13}C, glucose-5-^{13}C, and glucose-6-^{13}C. *P* values above figure indicate differences in ^{13}C among fragments and entire molecules with significant ^{13}C difference relative to ethanoate being marked with star (*) (repeated-measure ANOVA, df = 15,2, $P < 0.01$). Box plots indicate interquartile ranges with each line (from down to up) representing minimum, 25%, median, 75%, and maximum value, while dots represent outliers.

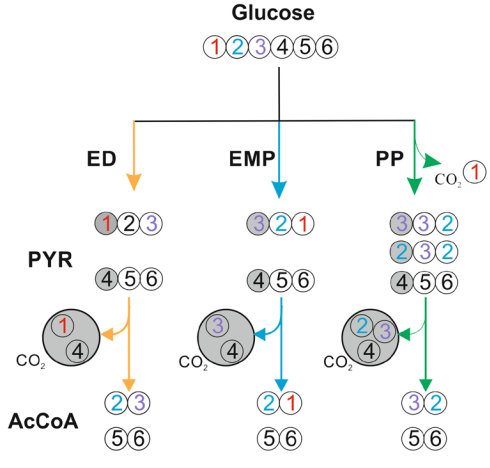

Fig. 2. Schematic representation of carbon incorporation from glucose into acetyl-CoA, the precursor for fatty acid biosynthesis. Carbon atom numbering for metabolites (pyruvate, PYR; acetyl-CoA, AcCoA) is ordered from left to right, while numbers indicate the C position in the original glucose molecule. ED indicates Entner-Doudoroff pathway, EMP is Embden-Meyerhof-Parnas glycolysis, and PP is pentose phosphate pathway. Gray background shading indicates those C positions released by pyruvate dehydrogenase as CO_2.

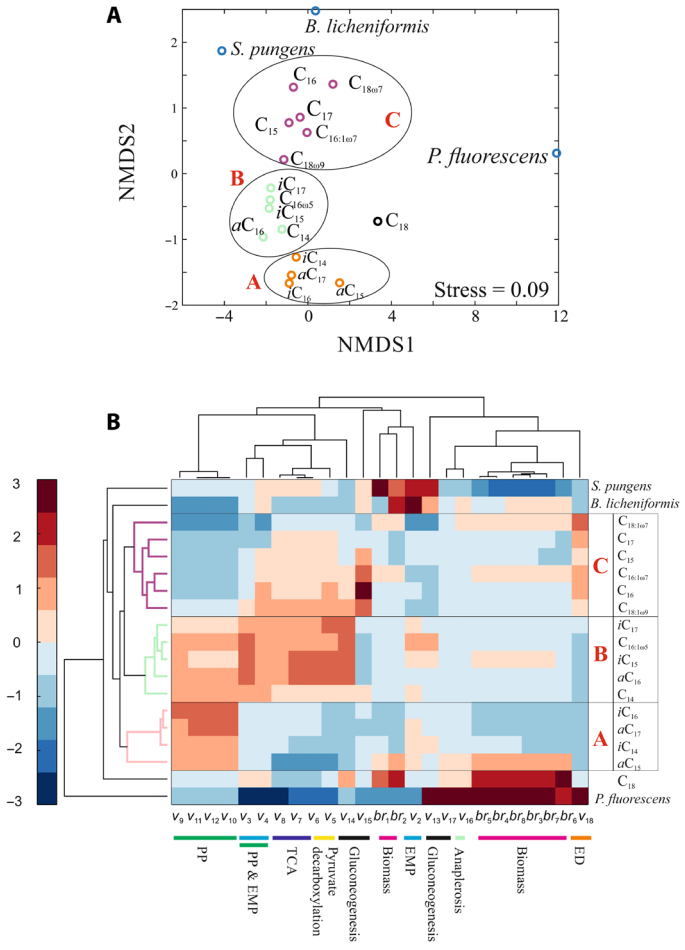

Fig. 3. Analysis of the metabolic flux patterns across PLFAs. NMDS (**A**) and cluster analysis of modeled central C metabolic fluxes (**B**) based on ^{13}C incorporation patterns into PLFA. To compare the observations with pure culture studies, the results for *B. licheniformis* and *P. fluorescens* from the study by Wu *et al.* (*20*) and *S. pungens* from the study by Scandellari *et al.* (*55*) are displayed (see the Supplementary Materials). Cluster analysis was based on the average Euclidean distance of fluxes between PLFAs. The heatmap shows the activity of the different pathways for individual PLFAs with red for pathway activities above and blue below the mean value. v_1 to v_{18} and br_1 to br_8 are reactions in the model of the central C metabolic network (fig. 1). TCA, tricarboxylic acid.

of Gram-positive bacteria (Fig. 3). Cluster B was mostly branched PLFAs but contained an unsaturated PLFA $C_{16:1\omega5}$ (Fig. 3), which was assigned to Gram-negative bacteria (*11*). It indicates that the Gram-negative bacteria that produce C16:1ω5 exhibit a metabolic pattern similar to Gram-positive bacteria. Using pure cultures, several studies showed similar high pentose phosphate pathway activity in Gram-negative *Escherichia coli* as in Gram-positive *Bacillus subtilis* (*6*, *23*).

Tricarboxylic acid cycle activity and CUE

Gram-positive and Gram-negative bacteria exhibited significant differences in the rates of the tricarboxylic acid cycle reactions (Kruskal-Wallis test, $P = 0.004 < 0.01$; Fig. 4B). Gram-positive cluster A bacteria had low reaction rates, while Gram-positive cluster B bacteria had high rates. Rates for Gram-negative bacteria were intermediate. Because of the strong negative correlation between the activity of the tricarboxylic acid cycle and CUE (Fig. 5), CUE was high for Gram-positive bacteria cluster A, intermediate for Gram-negative, and low for Gram-positive cluster B (Fig. 4C).

DISCUSSION

In this study, we used a PLFA-based metabolic flux analysis model to characterize the metabolic diversity within soil microbial community. The Entner-Doudoroff pathway has been suggested as an important alternative pathway for the Embden-Meyerhof-Parnas glycolysis for glucose catabolism (*24*–*26*). The high Entner-Doudoroff pathway activity in Gram-negative soil bacteria was consistent with findings that genes for Entner-Doudoroff are most prevalent in Gram-negative bacteria such as Proteobacteria, an important component of the soil microbiome (*27*, *28*). Moreover, PLFA iC_{17} and iC_{15}, representative for Gram-positive bacteria (*9*, *24*, *25*), showed significant but low Entner-Doudoroff pathway activity (table S2). Entner-Doudoroff pathway activity is rare in Gram-positive bacteria but has been observed, e.g., in *Enterococcus faecalis* and *Rhodococcus opacus* (*26*, *29*). It should be noted that iC_{17} and iC_{15} are also produced by mesophilic and anaerobic Gram-negative sulfate-reducing bacteria (*30*, *31*). However, these bacteria are unlikely to be abundant in agricultural soils.

Gram-negative *Pseudomonas* species almost always use the Entner-Doudoroff pathway (>90%) to catabolize glucose (*6*, *32*). High activity of the Entner-Doudoroff pathway is also found in marine bacteria (*33*), which were compared to terrestrial model bacteria, such as *E. coli*, *B. subtilis*, and *Corynebacterium glutamicum*. They

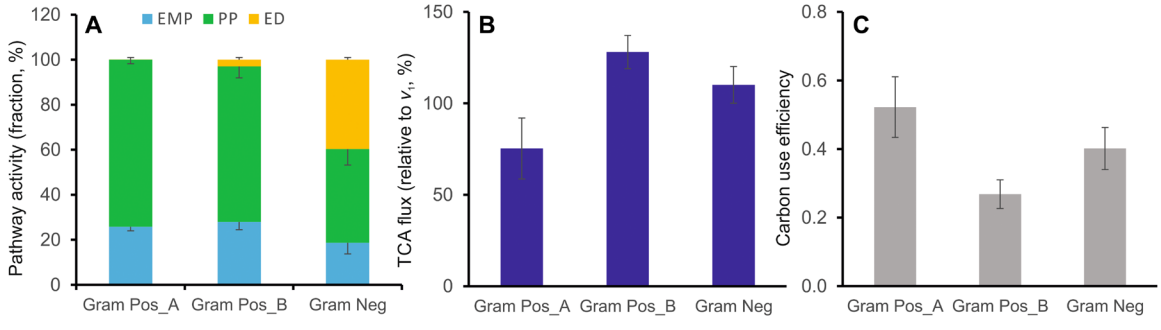

Fig. 4. Relative fluxes through the major metabolic pathways and carbon use efficiency of soil bacterial groups. Fraction of glucose directed to (**A**) Embden-Meyerhof-Parnas glycolysis and pentose phosphate and Entner-Doudoroff pathways, (**B**) flux rate of TCA cycle reaction (v_6) relative to the flux v_1 (glucose➔glucose-6-phosphate), and (**C**) CUE for cluster A, cluster B, and cluster C PLFAs. Means and SEs were calculated from the grouped PLFAs in Fig. 3.

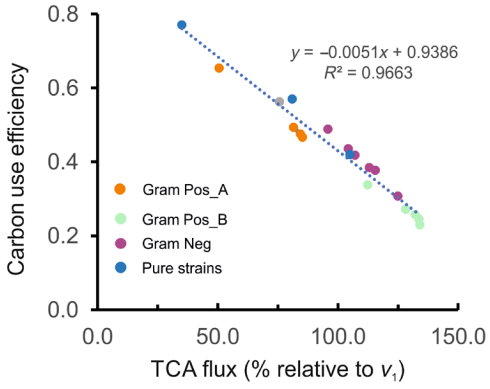

Fig. 5. Correlation between TCA cycle activity (v_6) and CUE. Each data point represents an individual PLFA in this study defining not only the correlation but also pure strains data (*20*, *55*) that are displayed in Fig. 3. Clusters A, B, and C are assigned as Gram-positive bacteria A (Gram Pos_A), Gram-positive bacteria B (Gram Pos_B), and Gram-negative bacteria (Gram Neg), respectively.

concluded that terrestrial bacteria exhibited predominantly a mix of Embden-Meyerhof-Parnas glycolysis and pentose phosphate pathway, while in marine bacteria, the Entner-Doudoroff pathway was dominant. However, we submit that Gram-negative bacteria in soil (this study) and likely in marine ecosystems (*33*) both exhibit strong Entner-Doudoroff pathway activity, while Gram-positive bacteria do not. High Entner-Doudoroff pathway activity is rather unexpected as it produces fewer adenosine 5′-triphosphate compared to Embden-Meyerhof-Parnas glycolysis. However, Entner-Doudoroff activity may be preferred because of lower protein cost and more favorable thermodynamic characteristics and because it yields NADPH (reduced form of nicotinamide adenine dinucleotide phosphate) that can be used to protect the cell from oxidative damage (*33*–*36*). In consequence, the unexpectedly high contribution of Entner-Doudoroff pathway to Gram-negative's metabolism in soil does not only underline the often observed strongly deviating functions of Gram-negative and Gram-positive microorganisms (*37*, *38*) in soil but also demonstrates that stress protection may be a major driver for the thermodynamics of the microbial metabolism and thus soil C transformations.

In laboratory studies, Gram-positive *Bacillus* species (e.g., *B. subtilis* and *B. licheniformis*) exhibited higher activity of Embden-Meyerhof-Parnas glycolysis (~70%) relative to pentose phosphate pathway (~30%) without a significant contribution of the Entner-Doudoroff pathway (*6*, *20*, *23*). In contrast, we observed a significantly higher activity of the pentose phosphate pathway than Embden-Meyerhof-Parnas glycolysis for both groups of Gram-positive bacteria in this soil community (two-tailed *t* test, *t* value = 9.9, df = 13, $P < 0.001$). This difference can be explained in two ways: (i) The limited set of bacterial isolates is not representative for most of the uncultivated Gram-positive bacteria in soil, or (ii) the environmental conditions in soil cause changes in pathway activity patterns. The latter may be related to the generally resource-limited environment of soil ecosystems (*39*) and soil Gram-positive bacteria being specialized for C-limited habitats in contrast to their growth conditions in pure cultures (*37*). Metabolic pathway activities are known to change under nutrient limitation (*5*, *7*, *40*). Similarly, changes in metabolic pathway activities were observed for whole soil communities in response to temperature (*13*), C availability (*16*), and presence of toxins (*41*). However, a high activity of pentose phosphate pathway and for Entner-Doudoroff pathway is associated with a high NADPH production, which may be a requirement to protect cells against oxidative damage in aerobic environments (*42*). Consequences of high pentose phosphate or Entner-Doudoroff pathway activity for the resistance and resilience of soil microbial communities to disturbances such as tillage or extreme droughts remain to be elucidated (*43*, *44*).

Microbes with high CUE are thought to be important for soil organic matter production and persistence, while microbes with low CUE are more likely the driver of a high soil respiration (*1*, *45*). However, evidence for variability in CUE within soil communities is mostly based on results from pure culture experiments (*10*, *12*, *45*, *46*). Sometimes oligotrophs are considered more efficient than copiotrophs (*47*), sometimes microbes investing less into resource acquisition are thought to be more efficient (*48*), or growth rate and CUE are negatively correlated (*21*). Variability in CUE has been experimentally demonstrated for an intact, complex microbial community under in situ conditions. Our results show that a diversity of glucose-processing biochemical pathways and variable CUE coexist under identical environmental conditions.

It is useful to compare our findings to genome-scale models (*10*, *12*). Our findings match observations of a high abundance of Entner-Doudoroff pathway genes for Gram-negative Proteobacteria (*9*). Moreover, we found significant but low Entner-Doudoroff pathway activity for Gram-positive bacteria in agreement with few observation of genes of this pathway in species of Firmicutes and Actinobacteria (*9*, *26*, *29*). Genome-based metabolic modeling has provided estimates of CUE that are strongly dependent on substrate used (*10*) but are difficult to scale to whole communities or groups of bacteria. Using soil fluxomics, we were able to provide initial experimental verification of these findings. However, more research is needed to bring these two approaches of fluxomics and genome-based modeling together. The close correlation between CUE and tricarboxylic acid cycle flux suggests that simplified proxies of the tricarboxylic acid cycle activity, potentially detected using metabolome analysis, might provide good estimates for CUE in complex microbiomes. Considering the moderate specificity of PLFAs (*15*, *19*), the analysis of further metabolites with biomarker function is required to improve the accuracy and coverage of fluxomics, to provide deeper insights of microbial identities, and to further align genome-based modeling and fluxomics. Because ^{13}C-PLFA–based stable isotope probing has been widely used to trace microbial activity and metabolism, our ^{13}C-PLFA–based metabolic flux analysis model aims to bring more insights into dynamic microbial metabolism even in low microbial activity or low microbial abundance environments.

Microbes play a crucial role in the production and consumption of soil organic matter. It has been proposed that a high CUE is beneficial for maintaining or even increasing soil C content (*49*, *50*), while a lowering of CUE could potentially reduce soil organic matter content (*2*). Knowing which microbial groups have a high CUE under in situ conditions could help identify which microbes contribute most to soil organic matter formation. This could lead to deeper insights into how changes in the environment affect soil C content and provide opportunities to optimize microbial communities with the purpose of increasing soil organic matter formation. Particularly in view of the "4 per 1000" (*51*), the development of agricultural management practices aimed at high CUE and thus improving soil C content is essential to mitigating climate change.

MATERIALS AND METHODS

Soil incubation with position-specific ^{13}C-labeled glucose

Samples of the upper 20 cm of an agricultural soil were collected from the "Campus Klein Altendorf" experimental station in Rheinbach, Germany (50°37′N, 6°59′E; Haplic Luvisol developed from loess) in May 2018. A detailed description of soil properties is given by Vetterlein *et al.* (*52*). Before incubation, bulk homogenized samples were sieved to 2 mm to remove plant debris and stored at 4°C for 1 month. About 10 g of field-moist soil (water content of ca. 20%) were transferred to 550-ml airtight glass jars. Soil samples (n = 2) were air-dried at room temperature overnight, after which 3 ml of glucose isotopomer stock solution (3.3 mg glucose ml^{-1}) was evenly spread over the soil surface with a pipette at a final concentration of 5.56 μmol glucose g^{-1} soil. The seven ^{13}C-labeled glucose isotopomers were glucose-1-^{13}C, glucose-2-^{13}C, glucose-3-^{13}C, glucose-4-^{13}C, glucose-5-^{13}C, glucose-6-^{13}C, and uniformly labeled glucose-U-$^{13}C_6$ (Sigma-Aldrich, >99 atomic % isotopic purity). Two control treatments were part of this experiment: 3 ml of Milli-Q water and 3 ml of natural abundance glucose addition (5.56 μmol glucose g^{-1} soil). The soil samples were incubated at 15°C for 10 days as previous (*53*).

PLFA extraction

About 8 g of lyophilized soil was extracted following a modified Bligh and Dyer method (*54*). PLFAs were purified on a solid-phase silica-gel extraction column eluted with chloroform, acetone, and methanol. After drying under N_2, PLFA were hydrolyzed with 0.5 ml of 0.5 M NaOH in methanol at 100°C for 10 min. After cooling to room temperature, 0.5 ml of 10% BF_3 in methanol was added, and the solution was incubated at 80°C for 15 min. Thereafter, 1 ml of saturated NaCl solution was added, and fatty acid methyl esters (FAMEs) were extracted four times with 2 ml of hexane. FAMEs were dried under N_2 and stored at −20 °C until further analysis.

Fragment ^{13}C analysis on GC-MS

FAMEs were detected on a GC 7890B connected to a single quadrupole mass spectrometer MSD 5977B (Agilent, Waldbronn, Germany). FAMEs were injected into the inlet at 280°C in splitless mode and separated on a DB-1 ms column (15 m in length, 0.25 mm in internal diameter, and 0.25 μm in film thickness) in tandem with a DB-5 ms column (same parameters as DB-1 ms but 30 m in length). The oven temperature program was 80°C (1 min) increased to 171°C at 10°C/min, increased to 192°C for 4 min at 0.7°C/min, followed by an increase to 206°C at 2°C/min and to 300°C for 10 min at 10°C/min. Electron ionization energy was set at 70 eV, and ion source and quadruple temperatures were kept at 230° and 150°C, respectively.

Full scan [mass charge ratio (m/z) 50 to 550 Da] and selected ion monitoring were used for qualitative measurements and isotope estimates, respectively. The selected m/z for the ethanoate and propionate fragments were molecular ions of FAME are listed in the Supplementary Materials. The PLFA used for metabolic flux modeling included iC$_{14}$, C$_{14}$, iC$_{15}$, aC$_{15}$, C$_{15}$, iC$_{16}$, aC$_{16}$, C$_{16:1\omega7}$, C$_{16:1\omega5}$, C$_{16}$, iC$_{17}$, aC$_{17}$, C$_{17}$, C$_{18:1\omega9}$, C$_{18:1\omega7}$, and C$_{18}$ and have been used for metabolic flux modeling of pure strains of *B. licheniformis* and *P. fluorescens* (*20*). The relative abundances of mass isotopomers were determined to calculate the ^{13}C atom percent excess (APE, atomic %) of the PLFA fragments and molecular ions after correcting for naturally occurring isotopes (Supplementary Materials) (*20*). More analysis details are available in the study by Wu *et al.* (*20*).

Metabolic flux modeling

The model of the central carbon metabolic network included the catabolic reactions of the pathways of Embden-Meyerhof-Parnas glycolysis, pentose phosphate pathway, Entner-Doudoroff pathway, tricarboxylic acid cycle, gluconeogenesis, and anaplerotic reactions as well as eight anabolic reactions for biomass synthesis (for more details, see fig. S1). ^{13}C APE of metabolites in the network was simulated using atom mapping matrices and label identification vectors. Assuming that the ethanoate fragment represents acetyl-CoA and the propionate fragment represents acetyl-CoA + acetyl-CoA C1 (C1 position of second acetyl) of the PLFAs, the differences between simulated acetyl and propyl isotope composition and that of the experimentally isotope composition of each PLFA were minimized using a nonlinear optimization algorithm (*20*). The objective function was as follows

$$\min f(v) = \sum_{i=1}^{n=6}[(\mathrm{APE\_eth}_i^{\mathrm{sim}} - \mathrm{APE\_eth}_i^{\mathrm{exp}}/\mathrm{APE\_eth}_U^{\mathrm{exp}})^2 + (\mathrm{APE\_pro}_i^{\mathrm{sim}} - \mathrm{APE\_pro}_i^{\mathrm{exp}}/\mathrm{APE\_pro}_U^{\mathrm{exp}})^2] \quad (1)$$

where $\boldsymbol{v}$ is the flux vector in metabolic stoichiometric network (see fig. S1), $\boldsymbol{i}$ (1 to 6) is the position in singly ^{13}C- labeled glucose that contains the ^{13}C tracer, and $\mathrm{APE\_eth}_i^{\mathrm{sim}}$, $\mathrm{APE\_pro}_i^{\mathrm{sim}}$, $\mathrm{APE\_eth}_i^{\mathrm{exp}}$, and $\mathrm{APE\_pro}_i^{\mathrm{exp}}$ are the simulated and experimentally determined APE of ethanoate and propionate, respectively, after the specific singly ^{13}C-labeled ($\boldsymbol{i}$) glucose. $\mathrm{APE\_eth}_U^{\mathrm{exp}}$ and $\mathrm{APE\_pro}_U^{\mathrm{exp}}$ are the experimentally determined APE of ethanoate and propionate of PLFA in the presence of uniformly ^{13}C-labeled glucose.

The CUE was estimated from CO_2 production (v_5, v_7, v_8, v_9, and v_{17}), CO_2 consumption (v_{16}), and glucose uptake (v_1) as follows

$$\mathrm{CUE} = 1 - (v_5 + v_7 + v_8 + v_9 + v_{17} - v_{16})/(6^* v_1) \quad (2)$$

The simulation of APE of metabolites and flux optimization was accomplished using MATLAB (2018b, MathWorks, USA) with the internal function fmincon. The precursor demand ratios for biomass synthesis (i.e., br_2 to br_8 in fig. S1) relative to br_1 were following Dijkstra *et al.* (*13*) and are provided in table S1. Three different precursor requirement ratios were used in modeling by assuming a relative abundance of microbial compositions of G^+, G^-, and fungi as 1:1:1, 4.5:4.5:1, and 1:1:8, respectively (*13*, *20*). The output results for the three modeled communities did not show significant differences (ANOVA, df = 2, 861, F = 0.030, P = 0.971). More details about the model script on MATLAB and underlying assumptions are available in the study by Wu *et al.* (*20*).

Statistics

Normal distribution was tested using a Kolmogorov-Smirnov test. Outliers were identified according to the 1.5× interquartile range rule in box-and-whisker plots. If the assumption of normal distribution was met, then a one-way ANOVA was used to test for significance, followed by a pairwise t test to compare the differences between two groups when significant differences were identified. When assumption of normal distribution was not met, a nonparametric Kruskal-Wallis test and pairwise Mann-Whitney U test were used. When an individual fatty acid was considered a single subject, repeated-measures ANOVA was used to test the ^{13}C difference among ethanoate, propionate, and molecular ion. If this ANOVA showed significances, then paired t tests were performed to further identify

significances between the fragments. The statistical analysis was accomplished using internal statistical functions in MATLAB (2018b, MathWorks, USA).

Hierarchical cluster analysis was used to group PLFAs on the basis of their modeled metabolic fluxes. To further validate the hierarchical cluster results and avoid the biases for the specific algorithms in hierarchal cluster analysis, NMDS was performed. Before analysis, the data were standardized using the z-score method by subtraction of the average and division by the SD, i.e., $z = (x - \bar{x})/\sigma$. Cluster analysis used the agglomerative hierarchical cluster method with average Euclidean distance for linkage. For NMDS analysis, stress values of <0.1 indicated a good ordination avoiding misleading interpretation. To compare our results, two pure strains *B. licheniformis* and *P. fluorescens* were from the study by Wu *et al.* (*20*), while the results for *Suillus pungens* were derived from the study by Scandellari *et al.* (*55*) but used the model in this study (more details in the Supplementary Materials).

SUPPLEMENTARY MATERIALS

Supplementary material for this article is available at https://science.org/doi/10.1126/sciadv.abq3958

View/request a protocol for this paper from *Bio-protocol*.

REFERENCES AND NOTES

1. R. L. Sinsabaugh, S. Manzoni, D. L. Moorhead, A. Richter, Carbon use efficiency of microbial communities: Stoichiometry, methodology and modelling. *Ecol. Lett.* **16**, 930–939 (2013).
2. S. B. Hagerty, K. J. van Groenigen, S. D. Allison, B. A. Hungate, E. Schwartz, G. W. Koch, R. K. Kolka, P. Dijkstra, Accelerated microbial turnover but constant growth efficiency with warming in soil. *Nat. Clim. Chang.* **4**, 903–906 (2014).
3. K. M. Geyer, E. Kyker-Snowman, A. S. Grandy, S. D. Frey, Microbial carbon use efficiency: Accounting for population, community, and ecosystem-scale controls over the fate of metabolized organic matter. *Biogeochemistry* **127**, 173–188 (2016).
4. P. Dijkstra, J. J. Dalder, P. C. Selmants, S. C. Hart, G. W. Koch, E. Schwartz, B. A. Hungate, Modeling soil metabolic processes using isotopologue pairs of position-specific ^{13}C-labeled glucose and pyruvate. *Soil Biol. Biochem.* **43**, 1848–1857 (2011).
5. M. Dauner, J. E. Bailey, U. Sauer, Metabolic flux analysis with a comprehensive isotopomer model in *Bacillus subtilis*. *Biotechnol. Bioeng.* **76**, 144–156 (2001).
6. T. Fuhrer, U. Fischer, E. Fau-Sauer, U. Sauer, Experimental identification and quantification of glucose metabolism in seven bacterial species. *J. Bacteriol.* **187**, 1581–1590 (2005).
7. T. Fürch, R. Hollmann, C. Wittmann, W. Wang, W.-D. Deckwer, Comparative study on central metabolic fluxes of Bacillus megaterium strains in continuous culture using ^{13}C labelled substrates. *Bioprocess Biosyst. Eng.* **30**, 47–59 (2007).
8. C. P. Long, M. R. Antoniewicz, High-resolution ^{13}C metabolic flux analysis. *Nat. Protoc.* **14**, 2856–2877 (2019).
9. J. N. Edirisinghe, P. Weisenhorn, N. Conrad, F. Xia, R. Overbeek, R. L. Stevens, C. S. Henry, Modeling central metabolism and energy biosynthesis across microbial life. *BMC Genomics* **17**, 568 (2016).
10. M. Saifuddin, J. M. Bhatnagar, D. Segrè, A. C. Finzi, Microbial carbon use efficiency predicted from genome-scale metabolic models. *Nat. Commun.* **10**, 3568 (2019).
11. B. W. Stone, J. Li, B. J. Koch, S. J. Blazewicz, P. Dijkstra, M. Hayer, K. S. Hofmockel, X.-J. A. Liu, R. L. Mau, E. M. Morrissey, J. Pett-Ridge, E. Schwartz, B. A. Hungate, Nutrients cause consolidation of soil carbon flux to small proportion of bacterial community. *Nat. Commun.* **12**, 3381 (2021).
12. L. A. Domeignoz-Horta, G. Pold, X.-J. A. Liu, S. D. Frey, J. M. Melillo, K. M. DeAngelis, Microbial diversity drives carbon use efficiency in a model soil. *Nat. Commun.* **11**, 3684 (2020).
13. P. Dijkstra, S. C. Thomas, P. L. Heinrich, G. W. Koch, E. Schwartz, B. A. Hungate, Effect of temperature on metabolic activity of intact microbial communities: Evidence for altered metabolic pathway activity but not for increased maintenance respiration and reduced carbon use efficiency. *Soil Biol. Biochem.* **43**, 2023–2031 (2011).
14. L. Zelles, Phospholipid fatty acid profiles in selected members of soil microbial communities. *Chemosphere* **35**, 275–294 (1997).
15. Å. Frostegård, A. Tunlid, E. Bååth, Use and misuse of PLFA measurements in soils. *Soil Biol. Biochem.* **43**, 1621–1625 (2011).
16. C. Apostel, M. A. Dippold, E. Bore, Y. Kuzyakov, Sorption of Alanine changes microbial metabolism in addition to availability. *Geoderma* **292**, 128–134 (2017).
17. E. K. Bore, S. Halicki, Y. Kuzyakov, M. A. Dippold, Structural and physiological adaptations of soil microorganisms to freezing revealed by position-specific labeling and compound-specific ^{13}C analysis. *Biogeochemistry* **143**, 207–219 (2019).
18. K. H. Orwin, I. A. Dickie, R. Holdaway, J. R. Wood, A comparison of the ability of PLFA and 16*S* rRNA gene metabarcoding to resolve soil community change and predict ecosystem functions. *Soil Biol. Biochem.* **117**, 27–35 (2018).
19. R. G. Joergensen, Phospholipid fatty acids in soil—Drawbacks and future prospects. *Biol. Fertil. Soils* **58**, 1–6 (2022).
20. W. Wu, P. Dijkstra, M. A. Dippold, ^{13}C analysis of fatty acid fragments by gas chromatography mass spectrometry for metabolic flux analysis. *Geochim. Cosmochim. Acta* **284**, 92–106 (2020).
21. D. A. Lipson, The complex relationship between microbial growth rate and yield and its implications for ecosystem processes. *Front. Microbiol.* **6**, 615 (2015).
22. A. Frostegård, E. Bååth, The use of phospholipid fatty acid analysis to estimate bacterial and fungal biomass in soil. *Biol. Fertil. Soils* **22**, 59–65 (1996).
23. R. S. Wijker, A. L. Sessions, T. Fuhrer, M. Phan, ^{2}H/^{1}H variation in microbial lipids is controlled by NADPH metabolism. *Proc. Natl. Acad. Sci. U.S.A.* **116**, 12173–12182 (2019).
24. K. Kersters, J. De Ley, The occurrence of the Entner-Doudoroff pathway in bacteria. *Antonie Van Leeuwenhoek* **34**, 393–408 (1968).
25. D. Kopp, A. Sunna, Alternative carbohydrate pathways–Enzymes, functions and engineering. *Crit. Rev. Biotechnol.* **40**, 895–912 (2020).
26. S. Z. Peykov, V. D. Aleksandrova, S. G. Dimov, Rapid identification of *Enterococcus faecalis* by species-specific primers based on the genes involved in the Entner-Doudoroff pathway. *Mol. Biol. Rep.* **39**, 7025–7030 (2012).
27. A. M. Spain, L. R. Krumholz, M. S. Elshahed, Abundance, composition, diversity and novelty of soil Proteobacteria. *ISME J.* **3**, 992–1000 (2009).
28. H.-S. Kim, S.-H. Lee, H. Y. Jo, K. T. Finneran, M. J. Kwon, Diversity and composition of soil Acidobacteria and Proteobacteria communities as a bacterial indicator of past land-use change from forest to farmland. *Sci. Total Environ.* **797**, 148944 (2021).
29. W. D. Hollinshead, W. R. Henson, M. Abernathy, T. S. Moon, Y. J. Tang, Rapid metabolic analysis of *Rhodococcus opacus* PD630 via parallel ^{13}C-metabolite fingerprinting. *Biotechnol. Bioeng.* **113**, 91–100 (2016).
30. F. Widdel, N. Pfennig, Studies on dissimilatory sulfate-reducing bacteria that decompose fatty acids. *Arch. Microbiol.* **129**, 395–400 (1981).
31. K. L. Londry, L. L. Jahnke, D. J. Des Marais, Stable carbon isotope ratios of lipid biomarkers of sulfate-reducing bacteria. *Appl. Environ. Microbiol.* **70**, 745–751 (2004).
32. M. Kohlstedt, C. Wittmann, GC-MS-based ^{13}C metabolic flux analysis resolves the parallel and cyclic glucose metabolism of *Pseudomonas putida* KT2440 and *Pseudomonas aeruginosa PAO1*. *Metab. Eng.* **54**, 35–53 (2019).
33. A. Klingner, A. Bartsch, M. Dogs, I. Wagner-Döbler, D. Jahn, M. Simon, T. Brinkhoff, J. Becker, C. Wittmann, H. Nojiri, Large-scale ^{13}C flux profiling reveals conservation of the Entner-Doudoroff pathway as a glycolytic strategy among marine bacteria that use glucose. *Appl. Environ. Microbiol.* **81**, 2408–2422 (2015).
34. A. Flamholz, E. Noor, A. Bar-Even, W. Liebermeister, R. Milo, Glycolytic strategy as a tradeoff between energy yield and protein cost. *Proc. Natl. Acad. Sci. U.S.A.* **110**, 10039–10044 (2013).
35. A. I. Stettner, D. Segrè, The cost of efficiency in energy metabolism. *Proc. Natl. Acad. Sci. U.S.A.* **110**, 9629–9630 (2013).
36. A. Stincone, A. Prigione, T. Cramer, M. M. C. Wamelink, K. Campbell, E. Cheung, V. Olin-Sandoval, N.-M. Grüning, A. Krüger, M. Tauqeer Alam, M. A. Keller, M. Breitenbach, K. M. Brindle, J. D. Rabinowitz, M. Ralser, The return of metabolism: Biochemistry and physiology of the pentose phosphate pathway. *Biol. Rev.* **90**, 927–963 (2015).
37. C. Kramer, G. Gleixner, Variable use of plant- and soil-derived carbon by microorganisms in agricultural soils. *Soil Biol. Biochem.* **38**, 3267–3278 (2006).
38. N. Fanin, P. Kardol, M. Farrell, M.-C. Nilsson, M. J. Gundale, D. A. Wardle, The ratio of Gram-positive to Gram-negative bacterial PLFA markers as an indicator of carbon availability in organic soils. *Soil Biol. Biochem.* **128**, 111–114 (2019).
39. J. L. Soong, L. Fuchslueger, S. Marañon-Jimenez, M. S. Torn, I. A. Janssens, J. Penuelas, A. Richter, Microbial carbon limitation: The need for integrating microorganisms into our understanding of ecosystem carbon cycling. *Glob. Chang. Biol.* **26**, 1953–1961 (2020).
40. E. Fischer, U. Sauer, A novel metabolic cycle catalyzes glucose oxidation and anaplerosis in hungry *Escherichia coli*. *J. Biol. Chem.* **278**, 46446–46451 (2003).
41. E. K. Bore, C. Apostel, S. Halicki, Y. Kuzyakov, M. A. Dippold, Soil microorganisms can overcome respiration inhibition by coupling intra- and extracellular metabolism: ^{13}C metabolic tracing reveals the mechanisms. *ISME J.* **11**, 1423–1433 (2017).
42. X. Chen, K. Schreiber, J. Appel, A. Makowka, B. Fähnrich, M. Roettger, M. R. Hajirezaei, F. D. Sönnichsen, P. Schönheit, W. F. Martin, K. Gutekunst, The Entner–Doudoroff pathway is an overlooked glycolytic route in cyanobacteria and plants. *Proc. Natl. Acad. Sci. U.S.A.* **113**, 5441–5446 (2016).

43. H. Yan, F. Yang, J. Gao, Z. Peng, W. Chen, Subsoil microbial community responses to air exposure and legume growth depend on soil properties across different depths. *Sci. Rep.* **9**, 18536 (2019).
44. R. Sun, W. Li, W. Dong, Y. Tian, C. Hu, B. Liu, Tillage changes vertical distribution of soil bacterial and fungal communities. *Front. Microbiol.* **9**, 699 (2018).
45. J. Lehmann, C. M. Hansel, C. Kaiser, M. Kleber, K. Maher, S. Manzoni, N. Nunan, M. Reichstein, J. P. Schimel, M. S. Torn, W. R. Wieder, I. Kögel-Knabner, Persistence of soil organic carbon caused by functional complexity. *Nat. Geosci.* **13**, 529–534 (2020).
46. S. D. Allison, M. D. Wallenstein, M. A. Bradford, Soil-carbon response to warming dependent on microbial physiology. *Nat. Geosci.* **3**, 336–340 (2010).
47. B. R. K. Roller, T. M. Schmidt, The physiology and ecological implications of efficient growth. *ISME J.* **9**, 1481–1487 (2015).
48. A. A. Malik, J. B. H. Martiny, E. L. Brodie, A. C. Martiny, K. K. Treseder, S. D. Allison, Defining trait-based microbial strategies with consequences for soil carbon cycling under climate change. *ISME J.* **14**, 1–9 (2020).
49. M. F. Cotrufo, M. D. Wallenstein, C. M. Boot, K. Denef, E. Paul, The Microbial Efficiency-Matrix Stabilization (MEMS) framework integrates plant litter decomposition with soil organic matter stabilization: Do labile plant inputs form stable soil organic matter? *Glob. Chang. Biol.* **19**, 988–995 (2013).
50. C. Liang, J. P. Schimel, J. D. Jastrow, The importance of anabolism in microbial control over soil carbon storage. *Nat. Microbiol.* **2**, 17105 (2017).
51. W. Amelung, D. Bossio, W. de Vries, I. Kögel-Knabner, J. Lehmann, R. Amundson, R. Bol, C. Collins, R. Lal, J. Leifeld, B. Minasny, G. Pan, K. Paustian, C. Rumpel, J. Sanderman, J. W. van Groenigen, S. Mooney, B. van Wesemael, M. Wander, A. Chabbi, Towards a global-scale soil climate mitigation strategy. *Nat. Commun.* **11**, 5427 (2020).
52. D. Vetterlein, T. Kühn, K. Kaiser, R. Jahn, Illite transformation and potassium release upon changes in composition of the rhizophere soil solution. *Plant and Soil* **371**, 267–279 (2013).
53. E. K. Bore, C. Apostel, S. Halicki, Y. Kuzyakov, M. A. Dippold, Microbial metabolism in soil at subzero temperatures: Adaptation mechanisms revealed by position-specific ^{13}C labeling. *Front. Microbiol.* **8**, 946 (2017).
54. A. Gunina, M. A. Dippold, B. Glaser, Y. Kuzyakov, Fate of low molecular weight organic substances in an arable soil: From microbial uptake to utilisation and stabilisation. *Soil Biol. Biochem.* **77**, 304–313 (2014).
55. F. Scandellari, E. A. Hobbie, A. P. Ouimette, V. K. Stucker, Tracing metabolic pathways of lipid biosynthesis in ectomycorrhizal fungi from position-specific ^{13}C-labelling in glucose. *Environ. Microbiol.* **11**, 3087–3095 (2009).
56. M. K. Hellerstein, R. A. Neese, Mass isotopomer distribution analysis at eight years: Theoretical, analytic, and experimental considerations. *Am. J. Physiol. Endocrinol. Metab.* **276**, E1146–E1170 (1999).
57. J. D. Young, INCA: A computational platform for isotopically non-stationary metabolic flux analysis. *Bioinformatics* **30**, 1333–1335 (2014).
58. L. He, S. G. Wu, M. Zhang, Y. Chen, Y. J. Tang, WUFlux: An open-source platform for ^{13}C metabolic flux analysis of bacterial metabolism. *BMC Bioinformatics* **17**, 444 (2016).
59. J. G. Hamilton, K. Comai, Rapid separation of neutral lipids, free fatty acids and polar lipids using prepacked silica sep-Pak columns. *Lipids* **23**, 1146–1149 (1988).
60. S. M. Heinzelmann, N. J. Bale, E. C. Hopmans, J. S. Sinninghe Damsté, S. Schouten, M. T. J. van der Meer, Critical assessment of glyco- and phospholipid separation by using silica chromatography. *Appl. Environ. Microbiol.* **80**, 360–365 (2014).

Acknowledgments: We thank X. Song, X. Zhang, B. Razavi, and K. Zamanian for the help with soil sampling. We also thank the ChemAxon Company for providing free academic software for isotopic distribution simulation. **Funding:** This work was carried out in the framework of the priority program 2322 "SoilSystems – System ecology of soils" funded by the DFG, project number DFG DI 2136/17-1. The contribution by P.D. was made possible by a USDA National Institute of Food and Agriculture Foundation Program (grant number, #2017-67019-26396), while that of B.A.H. by a grant from the U.S. Department of Energy's Biological Systems Science Division Program in Genomic Science DE-SCSC0020172. W.W. was supported by the National Natural Science Foundation of China (no. 42106046) and the European Union's Horizon 2020 Research and Innovation Programme under the Marie Sklodowska-Curie grant agreement no. 840240. **Author contributions:** The conceptualization was developed by W.W., P.D., and M.A.D. The experiment was performed by W.W. and L.S. All the authors analyzed, interpreted, and wrote the manuscript. **Competing interests:** The authors declare that they have no competing interests. **Data and materials availability:** All data needed to evaluate the conclusions in the paper can be found in the paper and/or the Supplementary Materials or accessed at https://doi.org/10.5281/zenodo.6934169. The MATLAB code of metabolic flux analysis model can be found at https://doi.org/10.1016/j.gca.2020.05.032.

Submitted 6 April 2022
Accepted 16 September 2022
Published 4 November 2022
10.1126/sciadv.abq3958